ACTA ONCOLOGICA
2023, VOL. 62, NO. 11, 1531–1535
https://doi.org/10.1080/0284186X.2023.2254924

Taylor & Francis
Taylor & Francis Group

LETTER TO THE EDITOR

Dose exposure to an adult present in the treatment room during pediatric pencil beam scanning proton therapy

Johannes Tjelta[a,b], Kristian Ytre-Hauge[b], Erlend Lyngholm[b], Andreas Handeland[a,b], Helge Henjum[b] and Camilla Stokkevåg[a,b]

[a]Department of Oncology and Medical Physics, Haukeland University Hospital, Bergen, Norway; [b]Department of Physics and Technology, University of Bergen, Bergen, Norway

ARTICLE HISTORY Received 25 May 2023; Accepted 29 August 2023

Introduction

Radiation protection regulations prohibit caretakers from remaining near patients or occupying the treatment room during radiotherapy. The International Commission for radiation protection (ICRP) [1] recommends a limited of effective doses of 20 mSv per year over a period of 5 years for radiation working personnel, and yearly 1 mSv set for the public. During conventional photon-based radiotherapy, studies have demonstrated exposure levels above the recommended limits [2–5]. Furthermore, ambient dose equivalent H*(10), which is a conservative estimate of effective dose using neutron fluence measurements in air, has been examined for passively scattered protons and has shown effective dose exposure per treatment Gy in the room to exceed the annual recommendations in the majority of the situations [6–8]. New treatment modalities such as pencil beam scanning (PBS) proton therapy (PT) may open new possibilities due to reduced radiation exposure in the treatment room [9].

During passively scattered PT the main contributor for producing neutrons is the treatment head, which generates 60-99% of the neutrons reaching the patient [10]. However, during PBS, the proton energy is primarily moderated near the cyclotron, i.e. further away from the patient and treatment room [11]. Subsequently, the beam traverses considerably less modifying components in the gantry and primarily interacts through monitor chambers having limited production of secondary particles [12]. In the treatment room, neutrons are therefore mainly produced within the patient during PBS. Through the commissioning of recent PBS facilities, including standardized irradiation of a water tank, H*(10) in the treatment room at 1–2.25 m at different angles has been measured to be well below the 1 mSv dose limit set by the ICRP [13–16]. Mares et al. [9] investigated H*(10) for an intracranial tumor with pediatric anthropomorphic phantoms of relevant age groups where all measurements in the treatment room fell below 1 mSv.

In-room dose exposure during delivery of modern PBS had decreased significantly compared to aged modalities such as passively scattered PT, with a lower expected dose burden to a person present either intentionally or unintentionally [9]. Whereas the previous studies have presented H*(10) surrounding proton treatment gantries, we have simulated the complete equivalent dose exposure to a tentative parent supporting a patient at different locations in the treatment room during realistic PBS treatment scenarios.

Materials and methods

Pediatric treatment plans

Two treatment plans were generated and optimized in the Eclipse (Varian Medical Systems, Palo Alto, California, US, artificial ProBeam360 data) one craniospinal irradiated (CSI, 1444 cc) patient and one patient with a low-grade glioma (brain tumor, 44 cc). The CSI patient was chosen for the extended treatment volumes, resulting in multiple required proton fields as well as the inclusion of a range shifter which both are known to influence the ambient dose [9,17]. The CSI patient plan included two lateral fields to the brain and three posterior fields to the spine, all with range shifters. The prescribed dose was 23.4 Gy (RBE) to the spinal cord and brain, with a maximum and minimum energy of 182 MeV and 87 MeV. The brain tumor patient was prescribed a dose of 54 Gy (RBE) with two lateral fields a maximum energy of 122 MeV and a minimum of 70 MeV. Both patients were 12 years old full-body-CT.

Treatment room implementation

Throughout this study, the FLUKA Monte Carlo (MC) code [18–20] was utilized for the recalculation of treatment plans optimized in the treatment planning system. A model of the PT treatment room under construction at Haukeland University Hospital (HUH) in Bergen, Norway was implemented in FLUKA. The components of the gantry influencing the in-room ambient neutron effective dose were included, as presented by Englbrecht et al. [21] in their examination of stray neutrons in a ProBeam treatment room. The parts of the gantry included were two coinciding cylinders, a gantry

CONTACT Johannes Tjelta Johannes.tjelta@uib.no Department of Oncology and Medical Physics, Haukeland University Hospital, Bergen, Norway; Department of Physics and Technology, University of Bergen, Bergen, Norway

cone, and an iron floor (Figure 1). As the ProBeam 360° does not have a counterweight this was not included. The treatment room was included according to drawings with walls, floor, and ceiling of concrete.

Monte Carlo simulation

The FLUKA MC code was used with its graphical user interface FLAIR [22] with the implemented DICOM module, enabling the use of CT images through conversion to a so-called voxel file with density and materials based on the CT Hounsfield Units. For the CSI patient, range shifters with a water equivalent thickness of 57 mm (5 cm PMMA) were also implemented in the simulations. One voxel file is simulated at a time, therefore the simulation was performed in two steps: During the first step, we simulated the treatment plan delivery for the patient and collected the phase space for protons, neutrons, and photons in the plane between the gantry side and parent side (Figure 1) of the treatment room for 10^9 primary protons per field. The phase space file contained the position, direction, energy, and type of particle. The phase space file was further used as a source for the second part of the simulation, where the parent was included at different positions in the treatment room, including a distance of 1 m from the isocenter (position 1, Figure 1), positioned at an angle of 45° 3 m from the isocenter (position 2) and lastly at 3 m from the isocenter (position 3). The three positions were chosen due to similar experimental with a difference in ambient dose equivalent [13,14,16]. For each position of the parent, each treatment field phase space data was used as a radiation source in the secondary simulation. Organs typically used for radiation-induced cancer risk calculations [23,24] were delineated for the parent, a grown male whole-body CT extracted from the cancer imaging archive [25]. We calculated absorbed and equivalent doses including all particles, where neutrons were weighted with the ICRP 103 model [1].

Results

Total particle fluence was reduced by a factor of 100 when exiting the patient and was reduced even further at the respective parent positions (Figure 1). Both photon patient spectra were similar, although the spectrum for the brain tumor patient had a slightly greater number of lower energy photons compared to the CSI patient (Figure 2). Both neutron spectra had an increase in neutron count for energies above 0.01 MeV and below 1 eV.

In both treatment scenarios, the mean body dose to the parent for the whole treatment was well below 1 mSv in all the considered positions. The CSI parent received 9.6 μSv, 4.8 μSv, and 2 μSv in positions 1, 2, and 3, respectively. During the simulated treatment of the brain tumor patient, the total parent mean body dose was 5.8 μSv, 1.8 μSv, and 1.2 μSv for the same positions. In both treatment scenarios, the parent was exposed to organ doses below 1 μSv/Gy. The difference between the patient plans was more prominent when investigating dose per treatment Gy, where the CSI parent received a dose of 0.4 μSV/Gy, 0.2 μSV/Gy and 0.09

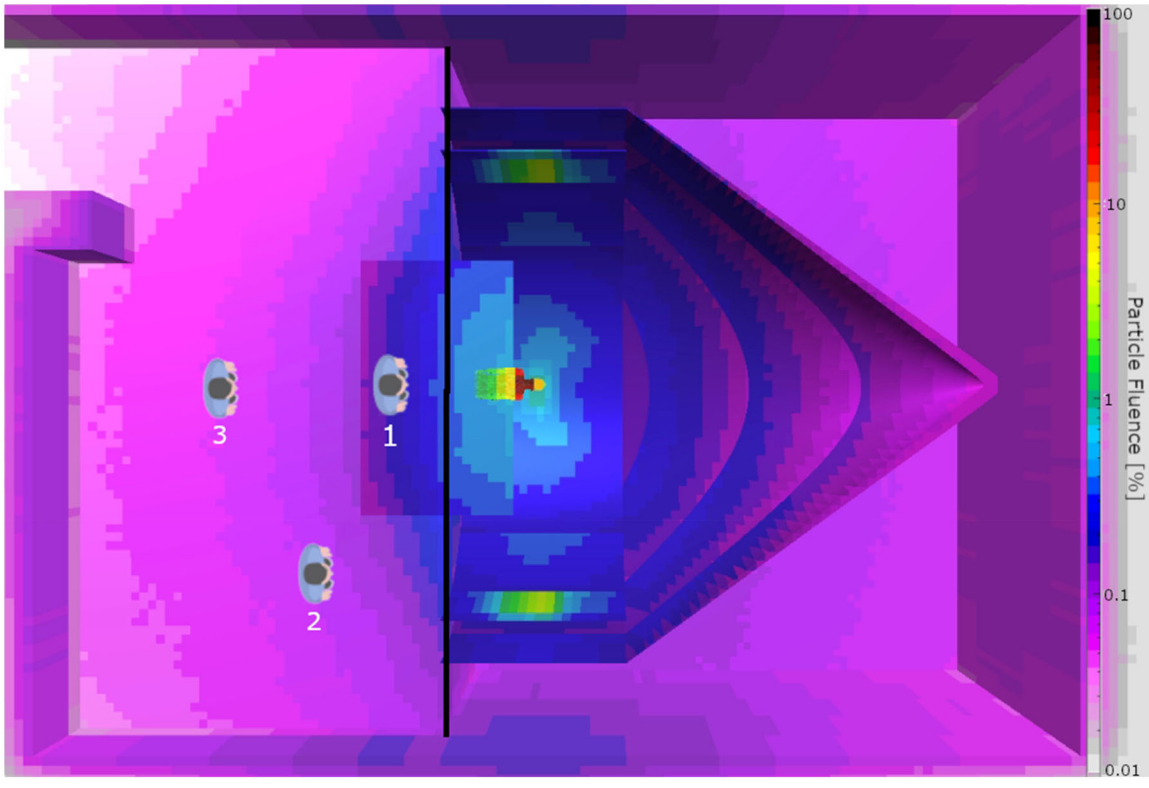

Figure 1. Particle fluence for all particles in the range 0.01 to 100% (normalized to maximum fluence in the tumor) for the CSI patient in the treatment room. The pediatric patient is situated in the gantry and the three positions for the parent in the treatment room are indicated (1: 1 m, 2: 3 m and 45°, 3: 3 m). The black line separating the patient and parent is the section sampling the phase space.

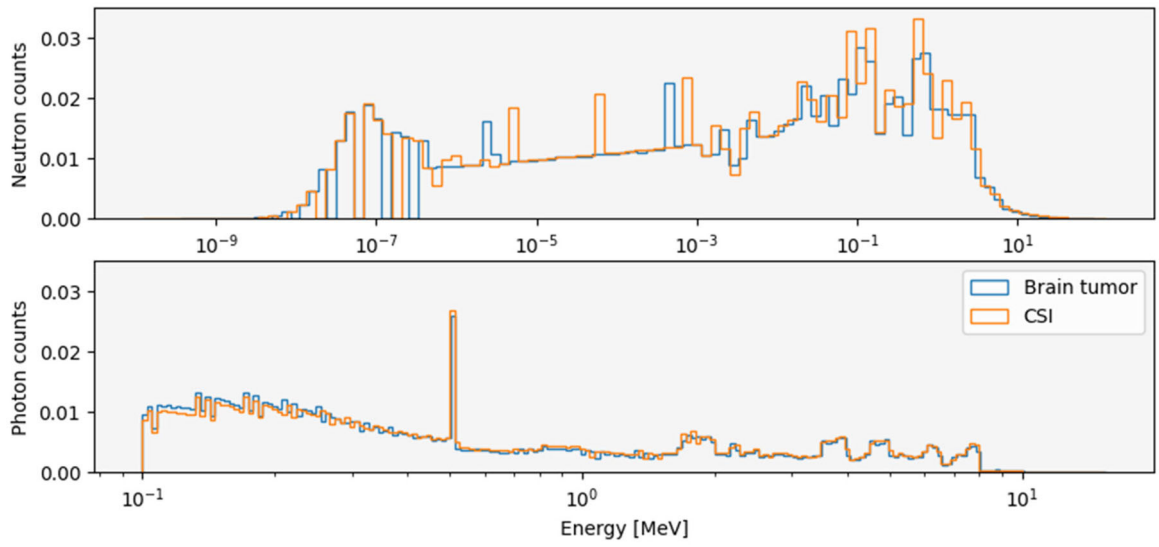

Figure 2. Neutron spectra (upper panel) and photon spectra (lower panel) for the brain tumor patient (blue lines) and CSI patient (orange lines). the spectra are calculated from the phase space energies collected during the simulations. All spectra are normalized such that the area under the curve equals to 1.

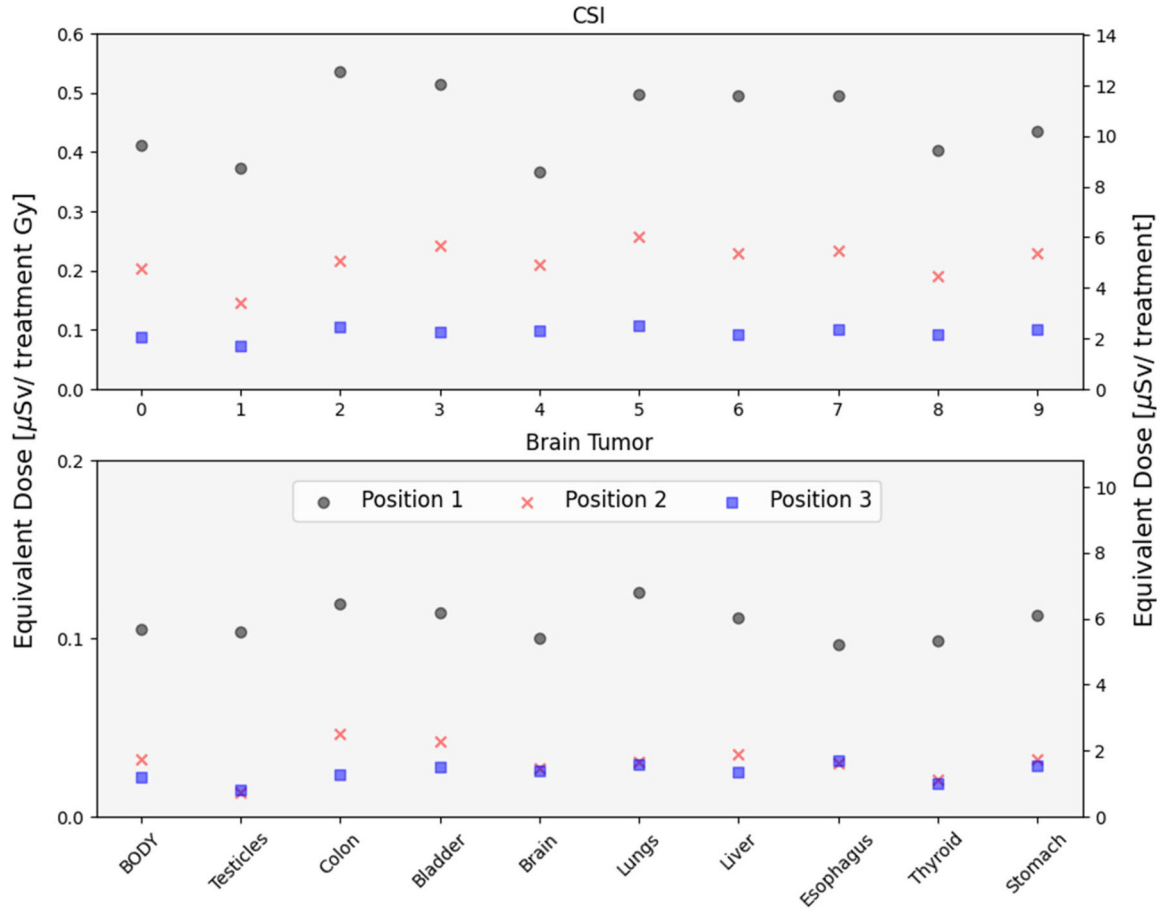

Figure 3. Organ mean equivalent dose received per treatment Gy for different organs and the whole-body of the CSI parent (upper panel) and brain tumor parent (lower panel). the upper panel is dose received for the CSI patient and the lower panel is for the brain tumor. In position 1 the parent is located 1 m from the iso-center (black circles), in position 2 at 45grader 3 m from the iso-center (red crosses) and in position 3 at a 3 m distance from the iso-center (blue squares).

μSV/Gy for positions 1, 2 and 3, whereas the brain tumor parent received 0.1 μSV/Gy, 0.04 μSV/Gy and 0.02 μSV/Gy (Figure 3). The most pronounced differences across organ doses were observed for the parent at position 1 for the CSI plan where the colon received a dose of 0.5 μSv/Gy. Organ dose differences for the brain tumor parent were negligible. When moving the parent from position 1 to 3 the dose decreased by a factor 4 (0.4 μSv/Gy to 0.1 μSv/Gy) for the CSI scenario and by a factor 5 (0.1 μSv/Gy to 0.02 μSv/Gy) for the brain tumor.

Discussion

The motivation behind this study was to examine the radiation exposure to a parent or caretaker present in a treatment room and to open a discussion related to reassessment of current radioprotection restrictions. The potential of having a parent present in the room during one or more of the treatment fractions could be comforting to a pediatric patient, and could potentially be a factor in reducing the use of anesthesia. For the two patient cases and parent positions examined, all doses for the whole treatment were below the recommended exposure limit of 1 mSv.

The patient case and parent position were found to influence the dose exposure, although other factors may also modify the exposure. Several groups have shown the contribution from secondary particles, mostly neutrons using ambient dose equivalent values (H*(10)). With a similar setup in the distance (1 m) and angle using bonner spheres, Trinkl et al. [16] measured a H*(10) of 0.2–5.2 μSv/Gy (neutrons) depending on the beam energy, Lillhok et al. [14] using TEPC detectors measured a total dose exposure (neutrons and photons) of 10 μSv/Gy. The two aforementioned studies used a water tank, Mares et al. [9] however, used an anthropomorphic phantom, with similar results to ours. Measurements of effective neutron dose parallel to the beam have been linked to an increased H*(10) per treatment Gy[10,16,26]. Even though the parent in our scenario for positions 2 and 3 had the same distance (3 m) to the isocenter, a total mean dose difference of 1–2 μSv was observed, depending on the patient case, presumably related to the angle relative to the proton beam. In addition, Trinkl et al. [16] showed as the proton beam increases from 140 MeV to 200 MeV the H*(10) increases significantly for all positions. The energies in our treatment plans did not exceed 179 MeV. In all, the energy, angle, tumor size, total dose delivered, patient size, inclusion of range shifters, and delivery method will all influence the dose exposure of the parent. To make a precise estimate for each treatment scenario, it would therefore be relevant to include both the specific treatment plan and accurate parent position. In addition, risk models from low-dose exposure, e.g., the BEIR VII report [23], could provide age- and gender-specific risk estimates. Notably, a grandparent would, for instance, have a lower risk compared to a parent, due to reduced risk with increasing age at exposure example as a LAR of 0.1% and 0.01% for a parent and grandparent receiving 1 mSv at age 45 and 70, furthermore a 0.01% difference in LAR between male and female with equal dose and age 45. In the dose modeling, we did not include activation of components, though it would contribute to the overall dose, it might be negligible compared to the equivalent dose a parent would receive directly [27–29]. Another contributor to dose exposure is adaptive planning with cone beam CT, which has been measured to be ~107 μSv 1 m from the iso center for a 5.1 mGy scan [30].

As no measurements have been obtained due to a construction treatment room, what components to include was determined by comparing to work done by Englbrecht et al. [21] Both neutrons spectra had an increase in amount for the low and high energy neutrons, similar to measurements [16,27] but an increase in intermediate neurons. The impact of neutrons and their weighting factors is a topic under discussion within radioprotection, where their maximum relative biological effectiveness (RBE_M) has been measured within ranges from 1 to 100 RBE_M[30,31]. The impact of the applied model for neutrons will thereby considerably affect the equivalent dose and subsequent radiation-induced cancer risk calculations. There are four strategies proposed in the literature, including the model from ICRP report 103[1], a lineal energy model by Baiocco et al. [32], a modified ICRP 60 model by Kellerer et al. [33], and an early model by United States Nuclear Regulatory Commission [34]. The latter two are older models and do not consider neutrons to be as biologically effective as the former two. Nevertheless, since neutrons and their biological effect are uncertain, the selected model could impact the result of dose calculations and risk for radiation-induced risk estimates.

Conclusion

Due to radioprotection regulations set in the past, caretakers are prohibited in the treatment room during beam-on time. Updated treatment modalities and delivery techniques, such as PBS, have reduced the exposure in the treatment room considerably. Current results indicate that the risks are low for a person occupying the treatment room intended or unintended during ongoing treatment. The presented results from common childhood cancer treatments, show that the exposure of a person is well below recommended limits and thereby encourage further studies of risks related to parents being present during treatment.

Acknowledgment

We wish to thank the Norwegian Childhood Cancer Society for funding this project

Disclosure statement

No potential conflict of interest was reported by the author(s).

Funding

This work was partly funded by Norwegian Childhood Cancer Society (210007) and The Norwegian Research Council (326218) Bioproton project. This work was supported by Barnekreftforeningen.

ORCID

Andreas Handeland http://orcid.org/0000-0002-6457-3954
Camilla Stokkevåg http://orcid.org/0000-0001-6352-4571

Data availability statement

The data that support the findings of this study are available from the corresponding author, JT, upon reasonable request.

References

[1] ICRP. The 2007 recommendations of the international commission on radiological protection. In: Valentin J, editor. Ann. ICRP. 2007. ICRP 37 (2-4).

[2] David S, Followill MSS, Kry SF, et al. Neutron source strength measurements for varian, siemens, elekta, and general electric linear accelerators. Sci Rep. 2003;4(3):6.

[3] Howell RM, Hertel NE, Wang Z, et al. Calculation of effective dose from measurements of secondary neutron spectra and scattered photon dose from dynamic MLC IMRT for 6 MV, 15 MV, and 18 MV beam energies. Med Phys. 2006; 33(2):360–368. doi: 10.1118/1.2140119.

[4] Kry SF, Salehpour M, Followill DS, et al. Out-of-field photon and neutron dose equivalents from step-and-shoot intensity-modulated radiation therapy. Int J Radiat Oncol Biol Phys. 2005; 62(4): 1204–1216. doi: 10.1016/j.ijrobp.2004.12.091.

[5] Lin JP, Liu WC, Lin CC. Investigation of photoneutron dose equivalent from high-energy photons in radiotherapy. Appl Radiat Isot. 2007;65(5):599–604. doi: 10.1016/j.apradiso.2007.01.017.

[6] Roy SC, Sandison GA. Scattered neutron dose equivalent to a fetus from proton therapy of the mother. Radiat Phys Chem. 2004;71(3–4):997–998. doi: 10.1016/j.radphyschem.2004.05.025.

[7] Han S-E, Cho G, Lee SB. An assessment of the secondary neutron dose in the passive scattering proton beam facility of the national cancer center. Nucl Eng Technol. 2017;49(4):801–809. doi: 10.1016/j.net.2016.12.003.

[8] Wroe A, Rosenfeld A, Schulte R. Out-of-field dose equivalents delivered by proton therapy of prostate cancer. Med Phys. 2007; 34(9):3449–3456. doi: 10.1118/1.2759839.

[9] Mares V, Farah J, De Saint-Hubert M, et al. Neutron radiation dose measurements in a scanning proton therapy room: can parents remain near their children during treatment? Front Oncol. 2022;12:903706. doi: 10.3389/fonc.2022.903706.

[10] Zacharatou Jarlskog C, Lee C, Bolch WE, et al. Assessment of organ-specific neutron equivalent doses in proton therapy using computational whole-body age-dependent voxel phantoms. Phys Med Biol. 2008;53(3):693–717. doi: 10.1088/0031-9155/53/3/012.

[11] van Goethem MJ, van der Meer R, Reist HW, et al. Geant4 simulations of proton beam transport through a carbon or beryllium degrader and following a beam line. Phys Med Biol. 2009; 54(19): 5831–5846. doi: 10.1088/0031-9155/54/19/011.

[12] Sawakuchi GO, Titt U, Mirkovic D, et al. Monte carlo investigation of the low-dose envelope from scanned proton pencil beams. Phys Med Biol. 2010; 55(3):711–721. doi: 10.1088/0031-9155/55/3/011.

[13] Lee S, Lee C, Shin EH, et al. Measurement of neutron ambient dose equivalent in proton radiotherapy with line-scanning and wobbling mode treatment system. Radiat Prot Dosimetry. 2017; 177(4):382–388. doi: 10.1093/rpd/ncx056.

[14] Lillhok J, Persson L, Andersen CE, et al. Radiation protection measurements with the variance-covariance method in the stray radiation fields from photon and proton therapy facilities. Radiat Prot Dosimetry. 2018; 180(1–4):338–341. doi: 10.1093/rpd/ncx194.

[15] Mojżeszek N, Farah J, Kłodowska M, et al. Measurement of stray neutron doses inside the treatment room from a proton pencil beam scanning system. Phys Med. 2017;34:80–84. doi: 10.1016/j.ejmp.2017.01.013.

[16] Trinkl S, Mares V, Englbrecht FS, et al. Systematic out-of-field secondary neutron spectrometry and dosimetry in pencil beam scanning proton therapy. Med Phys. 2017;44(5):1912–1920. doi: 10.1002/mp.12206.

[17] Yeom YS, Kuzmin G, Griffin K, et al. A Monte Carlo model for organ dose reconstruction of patients in pencil beam scanning (PBS) proton therapy for epidemiologic studies of late effects. J Radiol Prot. 2020;40(1):225–242. doi: 10.1088/1361-6498/ab437d.

[18] Böhlen TT, Cerutti F, Chin MPW, et al. The FLUKA code: developments and challenges for high energy and medical applications. Nucl Data Sheets. 2014;120:211–214. doi: 10.1016/j.nds.2014.07.049.

[19] Battistoni G, Bauer J, Boehlen TT, et al. The FLUKA code: an accurate simulation tool for particle therapy. Front Oncol. 2016;6: 116–139. doi: 10.3389/fonc.2016.00116.

[20] Ferrari Prs A, Fasso A, Ranft J. ′ FLUKA: a multi-particle transport code. CERN-2005-10; 2005.

[21] Englbrecht FS, Trinkl S, Mares V, et al. A comprehensive Monte Carlo study of out-of-field secondary neutron spectra in a scanned-beam proton therapy gantry room. Z Med Phys. 2021; 31(2):215–228. doi: 10.1016/j.zemedi.2021.01.001.

[22] Vlachoudis V. Flair: a powerful but user friendly graphical interface for FLUKA. United States: American Nuclear Society - ANS; 2009.

[23] National Research Council. Health risks from exposure to low levels of ionizing radiation: BEIR VII phase 2. Washington, DC: The National Academics Press; 2006. doi: 10.17226/11340.

[24] Schneider U, Sumila M, Robotka J. Site-specific dose-response relationships for cancer induction from the combined japanese A-bomb and hodgkin cohorts for doses relevant to radiotherapy. Theor Biol Med Model. 2011;8:27.

[25] Clark K, Vendt B, Smith K, et al. The cancer imaging archive (TCIA): maintaining and operating a public information repository. J Digit Imaging. 2013; 26(6):1045–1057. doi: 10.1007/s10278-013-9622-7.

[26] Antonie RH, Schneider U. Neutron dose and its measurement in proton therapy—current state of knowledge. BJR. 2019;93:1107–1119.

[27] Hanusova T, Johnova K, Navratil M, et al. Activation of QA devices and phantom materials under clinical scanning proton beams-a gamma spectrometry study. Phys Med Biol. 2018; 63(11):115014. doi: 10.1088/1361-6560/aac27f.

[28] Smith BR, Pankuch M, Hyer DE, et al. Experimental and monte carlo characterization of a dynamic collimation system prototype for pencil beam scanning proton therapy. Med Phys. 2020; 47(10):5343–5356. doi: 10.1002/mp.14453.

[29] Arjomandy B, Taylor P, Ainsley C, et al. AAPM task group 224: comprehensive proton therapy machine quality assurance. Med Phys. 2019; 46(8):e678–e705. doi: 10.1002/mp.13622.

[30] Ottolenghi A, Baiocco G, Smyth V, et al. The ANDANTE project: a multidisciplinary approach to neutron RBE. Radiat Prot Dosimetry. 2015; 166(1–4):311–315. doi: 10.1093/rpd/ncv158.

[31] Brenner DJ, Hall EJ. Secondary neutrons in clinical proton radiotherapy: a charged issue. Radiother Oncol. 2008; 86(2):165–170. doi: 10.1016/j.radonc.2007.12.003.

[32] Baiocco G, Barbieri S, Babini G, et al. The origin of neutron biological effectiveness as a function of energy. Sci Rep. 2016; 6(1): 34033. doi: 10.1038/srep34033.

[33] Kellerer AM, Leuthold G, Mares V, et al. Options for the modified radiation weighting factor of neutrons. Radiat Prot Dosimetry. 2004;109(3):181–188. doi: 10.1093/rpd/nch327.

[34] Standards for protection against radiation; final rule. In: commission NR., editor. Federal register: Nuclear Regelatory Commission; 1991.